Deletion of the P5abc Peripheral Element Accelerates Early and Late Folding Steps of the *Tetrahymena* Group I Ribozyme†

Rick Russell,* Pilar Tijerina, Amanda B. Chadee, and Hari Bhaskaran

Department of Chemistry and Biochemistry and Institute for Cellular and Molecular Biology, University of Texas, Austin, Texas 78712

Received September 27, 2006; Revised Manuscript Received February 15, 2007

ABSTRACT: The P5abc peripheral element stabilizes the *Tetrahymena* group I ribozyme and enhances its catalytic activity. Despite its beneficial effects on the native structure, prior studies have shown that early formation of P5abc structure during folding can slow later folding steps. Here we use a P5abc deletion variant ($E^{\Delta P5abc}$) to systematically probe the role of P5abc throughout tertiary folding. Time-resolved hydroxyl radical footprinting shows that $E^{\Delta P5abc}$ forms its earliest stable tertiary structure on the millisecond time scale, ∼5-fold faster than the wild-type ribozyme, and stable structure spreads throughout $E^{\Delta P5abc}$ in seconds. Nevertheless, activity measurements show that the earliest detectable formation of native $E^{\Delta P5abc}$ ribozyme is much slower (∼0.6 min^{-1}), in a manner similar to that of the wild type. Also similar, only a small fraction of $E^{\Delta P5abc}$ attains the native state on this time scale under standard conditions at 25 °C, whereas the remainder misfolds; footprinting experiments show that the misfolded conformer shares structural features with the long-lived misfolded conformer of the wild-type ribozyme. Thus, P5abc does not have a large overall effect on the rate-limiting step(s) along this pathway. However, once misfolded, $E^{\Delta P5abc}$ refolds to the native state 80-fold faster than the wild-type ribozyme and is less accelerated by urea, indicating that P5abc stabilizes the misfolded structure relative to the less-ordered transition state for refolding. Together, the results suggest that, under these conditions, even the earliest tertiary folding intermediates of the wild-type ribozyme represent misfolded species and that P5abc is principally a liability during the tertiary folding process.

Adoption of a specific three-dimensional structure for RNA is a complex process that typically involves the formation and accumulation of intermediates. Most fundamentally, this behavior arises because local RNA structure can form rapidly and can be stable in the absence of enforcing long-range or global structure, allowing partially structured intermediates to form and accumulate. The stability of RNA structure may lead, in general, to a hierarchy in its folding process, with global tertiary structure forming primarily from preformed units of secondary and local tertiary structure (*5*). This folding behavior contrasts with that of many proteins, whose local elements of secondary and tertiary structure are unstable in the absence of the global fold of a subunit or domain and are therefore formed in concert (*6*, *7*).

This hierarchy may facilitate the folding of RNAs, as stable structure that forms early can provide a scaffold upon which additional structure is built. However, hierarchical folding also introduces the possibility that incorrect structure will form and be stable, generating misfolded or "kinetically trapped" intermediates, which require partial or complete unfolding to continue folding productively. Indeed, RNA misfolding has been recognized since the early studies of tRNA (*8*, *9*) and has more recently been shown to be a near-ubiquitous feature of folding for large, multidomain RNAs (*10*−*16*).

A wealth of information on folding steps and intermediates has been obtained from studies of the *Tetrahymena* group I ribozyme. The ribozyme includes a core and several peripheral elements that surround the core. Several lines of evidence have indicated that one of the peripheral elements, termed P5abc, plays a vital role in folding. Time-resolved oligonucleotide hybridization and footprinting studies showed that tertiary folding begins with P5abc, followed closely by the rest of the P4−P6 domain (*2*, *3*, *17*, *18*) (Figure 1). The rest of the ribozyme then acquires stable structure through a series of intermediates (*2*, *3*, *18*), while P5abc and the entire P4−P6 domain retain structure in each subsequent intermediate. In addition to being the first subdomain to form, P5abc is the most stable part of the ribozyme, remaining ordered at the lowest Mg^{2+} concentration and the highest temperature (*19*, *20*). Consistent with the view of P5abc being a critical part of the structure, its deletion gives a ribozyme ($E^{\Delta P5abc}$)[1] that is substantially destabilized and has greatly diminished catalytic activity (*4*, *21*), defects that are rescued by addition of P5abc as a separate molecule (*4*, *22*). Because of its

† This work was supported by grants from the Welch Foundation (F-1563) and the National Institutes of Health (R01-GM070456) to R.R.

* To whom correspondence should be addressed. Telephone: (512) 471-1514. Fax: (512) 232-3432. E-mail: rick_russell@mail.utexas.edu.

[1] Abbreviations: DMS, dimethyl sulfate; EDTA, ethylenedinitrilotetraacetic acid; $E^{\Delta P5abc}$, *Tetrahymena* ribozyme variant lacking the P5abc peripheral element; PAGE, polyacrylamide gel electrophoresis; MOPS, 3-(*N*-morpholino)propanesulfonic acid; S, oligonucleotide substrate $CCCUCUA_5$; S*, 5′-^{32}P-labeled S.

10.1021/bi0620149 CCC: $37.00
Published on Web 04/10/2007

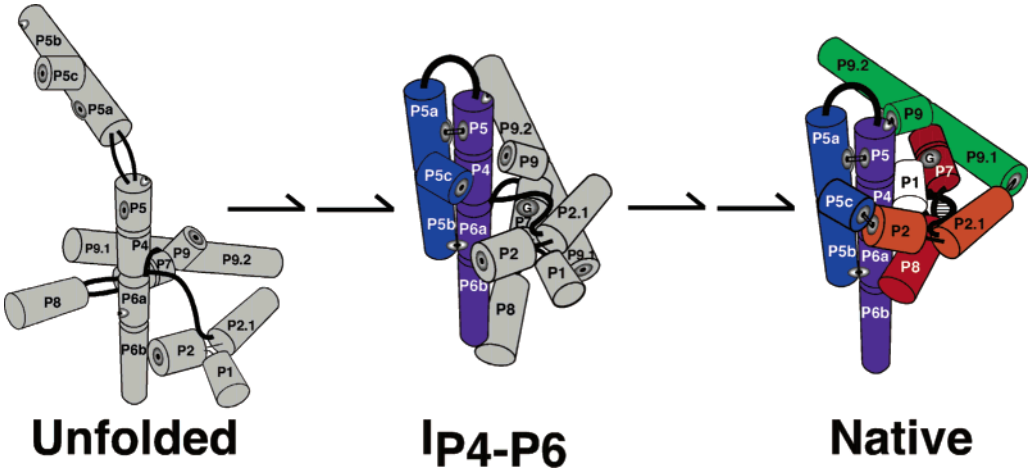

FIGURE 1: Tertiary folding of the *Tetrahymena* ribozyme. Double-stranded regions that do not have stable tertiary structure are shown as gray cylinders, and regions that have formed tertiary structure are colored as follows. The core domains, P4−P6 and P3−P8, are purple and red, respectively. The peripheral elements are P5abc (blue), P2/P2.1 (orange), and P9/P9.1/P9.2 (green). The species are separated by multiple arrows to emphasize the fact that additional intermediates are formed but not shown for the sake of simplicity. There are also additional pathways and misfolded species that are not shown (*15*, *18*, *41*) (see also Results and Figure 7).

stability and rapid formation of tertiary structure, P5abc was proposed to facilitate folding by nucleating formation of the P4−P6 domain, which would then provide the scaffold for the entire ribozyme (*3*, *23*).

On the other hand, studies of folding kinetics called into question the productive role of early P5abc folding. Several mutations that weaken native structure within P5abc increase the rate of formation of the stable tertiary structure within the P3−P8 domain, suggesting that native structure formed early within P5abc is transiently disrupted at a later stage of folding (*14*, *24*, *25*), and similar mutations accelerate refolding of a long-lived misfolded intermediate that is formed by most of the ribozyme population during folding (*26*; see also refs *15*, *27*, and *28*). Further, the small fraction of the ribozyme that avoids the misfolded conformation folds only slightly more slowly upon deletion of P5abc (*15*).

These studies indicated that under the conditions of these experiments (10 mM Mg^{2+} and <20 mM Na^{+}, "low-salt" conditions), the early formation of P5abc provides no overall benefit and even appears to slow folding steps involving the ribozyme core. However, it remained possible that P5abc accelerated early folding steps, but the beneficial effect was not detected because it was obscured by later steps that were unaffected or slowed by P5abc. More recently, it has been shown that mutation of a tertiary contact within P5abc or addition of the denaturant urea to the wild-type ribozyme accelerates even early folding steps, most simply suggesting that structure within P5abc is detrimental even early in folding (*29*).

To more fully understand the role of P5abc structure in folding, here we use footprinting and activity assays to systematically examine early and late folding steps, comparing folding of the wild-type ribozyme and the $E^{\Delta P5abc}$ variant under low-salt solution conditions. Strikingly, we find that deletion of P5abc accelerates even the early folding steps, suggesting that, under these conditions, most or all of the partially structured intermediates that accumulate are kinetically trapped. Further, although P5abc has little effect on the rate constant for native state formation along the sparsely populated pathway that avoids the long-lived misfolded conformation, it dramatically slows refolding of the heavily populated misfolded intermediate. Finally, we build on previous studies by showing that P5abc stabilizes the native state relative to partially structured and unstructured intermediates, supporting previous results in providing a rationale for its presence in the natural RNA even if the deleterious effects observed here are also present during folding in vivo.

MATERIALS AND METHODS

Materials. RNA and DNA oligonucleotides were from Dharmacon (Lafayette, CO) and IDT (Coralville, IA), respectively. Ribozymes were prepared as described previously (*30*, *31*). Ribozymes were labeled at the 5′ and 3′ ends as described previously (*30*, *32*, *33*). Oligonucleotides were labeled at the 5′ end as described previously (*30*). Unlabeled RNA was quantitated spectrophotometrically (*15*).

Time-Resolved Hydroxyl Radical Footprinting. Data were collected on beamline X-28C of the National Synchrotron Light Source (Brookhaven National Laboratory, Upton, NY) as described previously (*3*). The 5′- or 3′-^{32}P-labeled $E^{\Delta P5abc}$ ribozyme was incubated in CE buffer [10 mM sodium cacodylate (pH 7.5) and 0.1 mM EDTA] and loaded into a Kintek RQF-3 mixer positioned with a portion of its mixing loop in the path of the X-ray beam. Folding was performed at 42 °C in 10 mM Mg^{2+} for various times (from 10 ms to 180 s) before exposure to the X-ray beam (50 ms). Irradiated samples were precipitated with ethanol, resolved by 8% denaturing PAGE, and visualized on a phosphorimager. Band intensities were quantitated using SAFA (*34*) with limited RNase T1 digestions to assign bands.

Fe(II)-EDTA Footprinting. ^{32}P-labeled $E^{\Delta P5abc}$ ribozyme (20 000 cpm/μL, <10 nM) was folded predominantly to the misfolded conformation by incubation in 50 mM Na-MOPS (pH 7.0) and 10 mM Mg^{2+} at 25 °C for 10 min. P5abc was then added, if desired, to a final concentration of 200 nM. Native ribozyme was generated by incubating the mixture at 50 °C for 30 min under the same solution conditions in the presence of P5abc (*33*). For all reactions, $^{1}/_{10}$ volume of Fe(II)-EDTA reagent was added [final concentrations of 2 mM $(NH_4)_2Fe(II)(SO_4)_2$, 2.5 mM Na-EDTA, and 6 mM sodium ascorbate], and footprinting reaction mixtures were

incubated for 10 min at 25 °C. Reactions were quenched with 33 mM thiourea and 30% formamide and processed as described above.

DMS Footprinting. Misfolded and native ribozyme were prepared as described above. Footprinting was performed at 25 °C as described previously (*26*, *35*) [2 μM ribozyme, 50 mM Na-MOPS (pH 7.0), and 10 mM $MgCl_2$]. Reverse transcription products were separated via 8% denaturing PAGE and quantitated manually using ImageQuant (Amersham).

Measurement of Initial Folding Rates by Enzymatic Activity. Tertiary folding was initiated by adding Mg^{2+} (typically 10 mM) under the desired conditions [25 or 42 °C in 50 mM Na-MOPS (pH 7.0) or 10 mM sodium cacodylate (pH 7.5)]. Aliquots were "quenched", i.e., blocked from formation of additional native ribozyme, by being transferred to 0 °C and adding 50 mM Mg^{2+}, 500 nM P5abc, and 500 μM guanosine (see Figure S2 of the Supporting Information). The fraction of native ribozyme was then determined by adding ^{32}P-labeled substrate (S*, <2 nM) and following its cleavage. S* is bound by base pairing with the native ribozyme and folding intermediates, but it is only cleaved by the native ribozyme (*28*). Therefore, the fraction that is cleaved in a burst provides a good measure of the fraction of ribozyme present in the native state (*28*). Cleavage reactions were quenched with 2 volumes of 70% formamide, 100 mM EDTA, 0.1% bromophenol blue, and 0.1% xylene cyanol and analyzed via 20% denaturing PAGE (*15*, *30*, *36*). Data were fit by eq 1

$$\text{fraction P*} = A_1(1 - e^{-k_1 t}) + A_2(1 - e^{-k_2 t}) \qquad (1)$$

where A_1 is the fraction of the substrate that is cleaved rapidly with the rate constant k_1. The parameter A_1 was then plotted against folding time (t_1 in Figure 3A) to produce the plots in panels B and C of Figure 3 (see Figure S2C of the Supporting Information for full cleavage reactions).

Refolding of the Long-Lived Misfolded Conformer of the $E^{\Delta P5abc}$ Ribozyme. Native ribozyme formation was followed by enzymatic activity, analogous to experiments described above except that here the low-temperature incubation is not used; folding is instead quenched by adding Mg^{2+} to a final concentration of 50 mM at 25 °C (*26*, *28*, *33*). The low-temperature quench is unnecessary because the misfolded conformation is sufficiently long-lived that its refolding can be arrested at higher temperatures (*33*). (The low-temperature quench, although unnecessary, gives the same results within error; compare Figures 3C and 5A.) $E^{\Delta P5abc}$ (from 200 nM to 1 μM) was first incubated to generate misfolded ribozyme (25 °C in 10 mM Mg^{2+} for 10 min). The solution conditions were then changed if desired, and aliquots were blocked from further refolding after various times by addition of 250 nM P5abc, 500 μM guanosine, and 50 mM Mg^{2+} at 25 °C (*33*). S* was added for 1 min to determine the amount of native native ribozyme from the fraction of substrate cleaved rapidly.

Measurement of the Mg^{2+} Dependence for Formation of the Native Ribozyme. $E^{\Delta P5abc}$ ribozyme (100 nM) was incubated with Mg^{2+} (0−20 mM Mg^{2+} at 25 °C and pH 7.0) for 2 h to allow equilibration of the native species and folding intermediates. This incubation is expected to be sufficient because the half-life for equilibration of the native and long-lived misfolded species is ~30 min at 10 mM Mg^{2+} (see Figure 5) and is expected to be even shorter at lower Mg^{2+} concentrations (*28*), and transitions between any other folded and unfolded species are at least as fast (*33*). Additional Mg^{2+} (50 mM) and P5abc (500 nM) were then added to restore catalytic activity, allowing determination of the fraction of native ribozyme present during the initial incubation. After a 10 min incubation to allow P5abc binding and folding of unfolded ribozyme (predominantly to the misfolded species; see Figures 3 and 7), guanosine was added to a final concentration of 500 μM and S* was added for 1 min. Reactions were quenched and mixtures processed as described above.

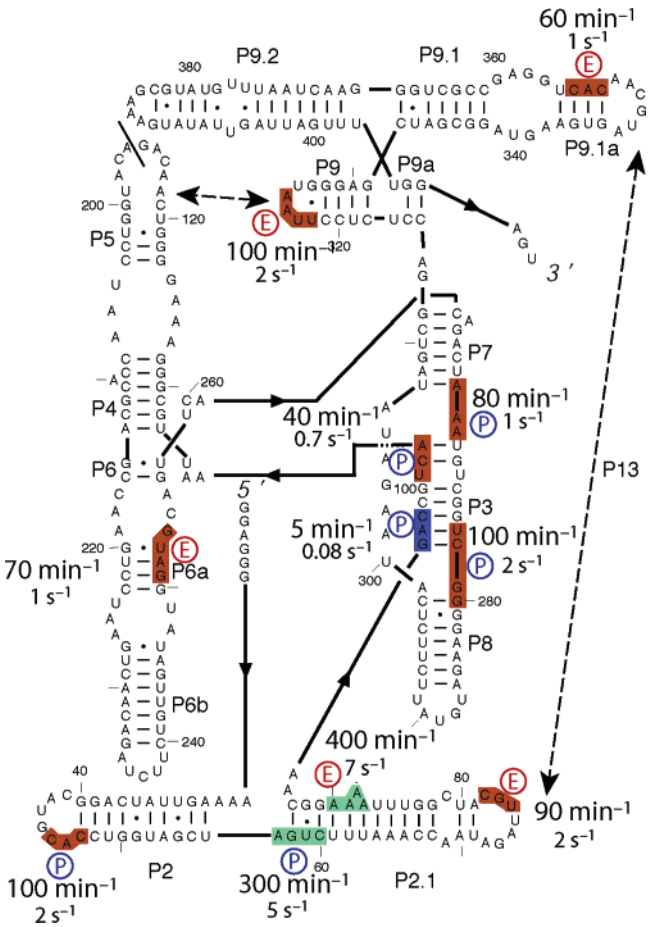

FIGURE 2: Time-resolved footprinting of $E^{\Delta P5abc}$ ribozyme folding. Regions that undergo a change in exposure to hydroxyl radicals are shown on the ribozyme secondary structure, along with the corresponding rate constants, and are color-coded by rate constant. Colors are green for >150 min^{-1}, orange for 40−150 min^{-1}, and purple for <40 min^{-1}. The color scheme is modeled after that used previously for the wild-type ribozyme (*3*). Regions marked with a blue P are protected in the folded structure relative to the unfolded structure, and regions marked with a red E are enhanced in the folded structure. Conditions: 42 °C, 10 mM sodium cacodylate, pH 7.5, and 10 mM $MgCl_2$.

RESULTS

Acceleration of Early Folding Steps upon Deletion of P5abc. To explore the effects of P5abc on early folding steps, we used X-ray-dependent hydroxyl radical footprinting to follow folding of the $E^{\Delta P5abc}$ ribozyme under conditions used previously for the wild-type ribozyme [42 °C, 10 mM sodium cacodylate, pH 7.5, 10 mM Mg^{2+} (*2*, *3*)]. Like the wild-

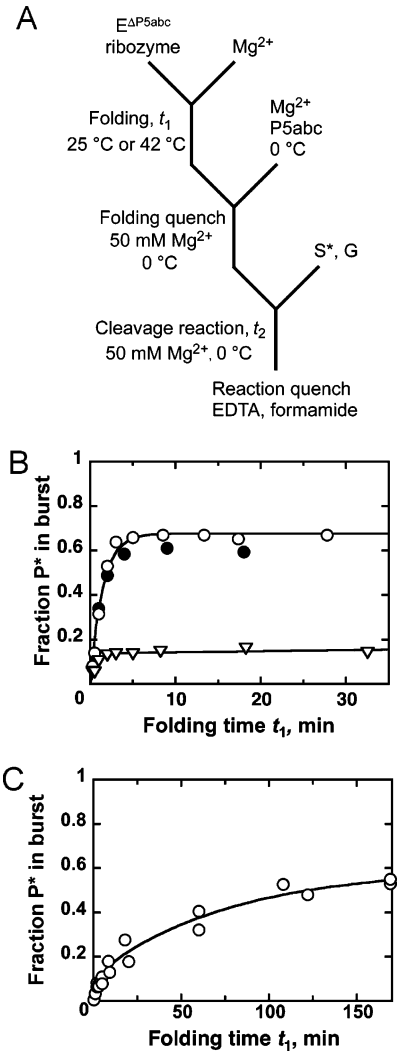

FIGURE 3: Monitoring initial folding by activity. (A) In the reaction scheme, folding is initiated by addition of Mg^{2+} for time t_1 before being arrested by the transfer of the sample to 0 °C and addition of higher Mg^{2+} concentrations and P5abc. The fraction of ribozyme present in the native state at the time of the transfer is then determined by measuring the fraction of input S* that is rapidly cleaved during t_2. (B) Progress of ribozyme folding to the native state. White circles show folding of $E^{\Delta P5abc}$ under footprinting conditions, and black circles show folding of $E^{\Delta P5abc}$ at 42 °C in 50 mM Na-MOPS (pH 7.0). The equilibrium fractions of the native ribozyme reported in the text were calculated by dividing the end point of the curve by the maximal end point, 0.85 (*33*), with the remaining 0.15 presumably representing the damaged ribozyme. Triangles show folding of the wild type under footprinting conditions. The slower phase, representing refolding of the misfolded ribozyme and not detectable on the time scale shown, gave a rate constant of $\sim 10^{-3}$ min^{-1}. (C) $E^{\Delta P5abc}$ ribozyme folding under conditions that give accumulation of misfolded ribozyme (25 °C, 50 mM Na-MOPS, pH 7.0, and 10 mM Mg^{2+}).

type ribozyme, groups of nucleotides throughout the ribozyme core and periphery changed in their accessibility to hydroxyl radicals upon addition of Mg^{2+} (Figure 2 and Figure S1 of the Supporting Information). Nearly all of the groups overlapped with those that are protected during folding of the wild-type ribozyme (*2*, *3*), suggesting that $E^{\Delta P5abc}$ folds to a globally similar structure. Only a subset of the wild-type protections were observed for $E^{\Delta P5abc}$, as expected from the large interface of P5abc with the ribozyme body (*37*) and consistent with previous equilibrium footprinting experiments with $E^{\Delta P5abc}$ (*21*). An additional difference was that several regions were enhanced in reactivity, rather than protected, in the folded $E^{\Delta P5abc}$ ribozyme. Although enhancements were not noted in earlier time-resolved footprinting studies, they were observed in recent equilibrium footprinting of the wild-type ribozyme in the same regions (*26*). The enhanced regions are all expected to be solvent-exposed in the folded $E^{\Delta P5abc}$ ribozyme (*38*) and presumably become more exposed upon folding because they transiently adopt positions in the unfolded ensemble that give at least weak protection from solvent.

The protections and enhancements occurred over a range of time scales, and data from each group of contiguous nucleotides were described adequately by a single rate constant.[2] In contrast to the wild-type ribozyme, for which the most rapid changes were localized within the P4−P6 domain, the earliest changes for the $E^{\Delta P5abc}$ ribozyme were outside P4−P6, near the junction of P2 and P2.1. These changes gave rate constants of 300−400 min^{-1} (5−7 s^{-1}), larger than any for the wild type under these conditions (*2*, *3*). Further changes then appeared throughout $E^{\Delta P5abc}$ with rate constants of 40−100 min^{-1} (0.6−2 s^{-1}), the same time scale as the most rapid changes for the wild type. These changes included most of the periphery (L2, L2.1, L9, and P9.1a)[3] and the core (P6a, P7, P8, and P3). Thus, under these conditions, $E^{\Delta P5abc}$ achieves stable formation of its global tertiary structure substantially faster than the wild-type ribozyme.

Although nearly all of the changes in accessibility were complete within a few seconds, one was substantially slower; nucleotides 96−98 of P3 were protected at 5 min^{-1} (0.08 s^{-1}). The slowest protections for the wild type are also within P3 under these conditions (*2*, *3*), suggesting that reorganization of the core occurs in a slow step for both ribozymes (*27*, *39*). However, unlike the wild type, for which the slowest changes occur simultaneously with the earliest formation of the native ribozyme (*3*, *15*, *17*), the slowest change observed here for $E^{\Delta P5abc}$ is 5−10-fold faster than the earliest appearance of the native state (see below), implying that the slowest folding steps do not give detectable changes in the footprinting pattern.

Initial Formation of the Native $E^{\Delta P5abc}$ Ribozyme. To monitor the effect of P5abc on later folding steps, we followed the formation of the native ribozyme by measuring the onset of enzymatic activity (*15*, *17*, *28*). It was shown previously that, at high Mg^{2+} concentrations and slightly lower temperatures (50 mM Mg^{2+}, 37 °C), $E^{\Delta P5abc}$ folds to the native state with a rate constant similar to that of the most rapid phase of native state formation for the wild-type

[2] Under some conditions, the wild-type ribozyme gives multiple rate constants and bursts for some regions (<60 ms) (*1*, *2*). Comparison of our time-resolved data with patterns of 5′-labeled ribozyme in the absence of Mg^{2+} did not provide evidence of bursts (data not shown), nor did any groups of residues necessitate multiple rate constants. However, the uncertainty is such that we cannot rule out bursts with small amplitudes (see Figure S1 of the Supporting Information). Because the wild type does not display bursts under these conditions (*2*, *3*), bursts for $E^{\Delta P5abc}$ would strengthen the conclusion that P5abc slows early folding steps.

[3] Protection within L2 was surprising because its tertiary contact partner, L5c, is not present in $E^{\Delta P5abc}$. Thus, the protection apparently arises from formation of structure within the loop or from a non-native tertiary contact of the loop. These nucleotides were protected on the same time scale in the wild type (*2*), suggesting that the same transition gives protection in both ribozymes.

ribozyme [0.4 min^{-1} for $E^{\Delta P5abc}$ and 0.9 min^{-1} for the wild type (*15*)]. Folding of $E^{\Delta P5abc}$ was followed only at high Mg^{2+} concentrations, because at lower Mg^{2+} concentrations its cleavage reaction is slower than folding (*4*), and therefore, an analogous experiment would not provide a measure of the folding rate.

To allow a broader exploration of conditions and to integrate results with those from footprinting, we sought conditions that would effectively block folding on the experimental time scale but would allow substrate cleavage (Figure 3A). Then we could monitor folding under any set of conditions using a discontinuous assay by transferring aliquots of a folding reaction to these "folding quench" conditions and then determining the fraction of native ribozyme by measuring the fraction that is enzymatically active (*28*, *33*). We found that 0 °C, 50 mM Mg^{2+}, and 500 nM P5abc RNA provided an effective folding quench (Figure S2 of the Supporting Information). First, when we started from the unfolded ribozyme, no native ribozyme was detectable for >150 min under the conditions of the folding quench, indicating that folding is effectively blocked. Second, ribozyme preincubated with P5abc to form the native state gave rapid substrate cleavage (0.7 min^{-1}) under the quench conditions.[4] To confirm that this assay accurately measures the rate of folding to the native state, we assessed folding of the $E^{\Delta P5abc}$ and wild-type ribozymes under conditions that also allow the use of the published continuous assay [in which Mg^{2+} and substrate are added simultaneously (*28*)] and obtained similar results with the two methods (Figure S3 of the Supporting Information).

We then used the discontinuous assay to follow folding of $E^{\Delta P5abc}$ under conditions that were previously inaccessible. Under the footprinting conditions, the native ribozyme appeared with a single rate constant of 0.75 ± 0.10 min^{-1} and an end point of ~80% (Figure 3B). This transition is 5−10-fold slower than the slowest change detected by footprinting (5 min^{-1}, Figure 2). The ~80% end point indicates that not all of the $E^{\Delta P5abc}$ ribozyme achieves the native state, consistent with the previous finding that it equilibrates between the native species and a long-lived misfolded species under similar conditions (*33*). The equilibrium fraction of native ribozyme is somewhat higher here (0.6 previously), suggesting that the higher temperature or changes in solution conditions stabilize the native structure modestly (10 mM sodium cacodylate buffer here, 50 mM Na-MOPS buffer previously). A reaction in MOPS buffer at 42 °C produced similar behavior and an intermediate fraction of the native ribozyme at equilibrium (0.72, Figure 3B), suggesting that higher temperature and the cacodylate buffer conditions each stabilize the native state somewhat relative to the misfolded state.

Scheme 1

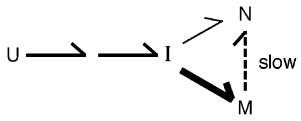

Under the conditions of the footprinting experiments, the native wild-type ribozyme appeared with a similar rate constant [1.3 ± 0.2 min^{-1} (Figure 3B)]. However, folding was biphasic, with only a small fraction of the ribozyme reaching the native state in this initial process. This low fraction was expected, as it was shown previously that the ribozyme partitions during folding to give predominantly a long-lived misfolded conformation under similar conditions, which slowly refolds to the native state (Scheme 1, where U, M, and N refer to unfolded, misfolded, and native ribozyme, respectively, and I is a folding intermediate; see refs *15*, *25*, and *28* and Figure 7). The accumulation of a large fraction of misfolded ribozyme for the wild-type but not the $E^{\Delta P5abc}$ ribozyme suggests either that the $E^{\Delta P5abc}$ ribozyme does not populate a long-lived misfolded species under these conditions, implying a change in the predominant folding pathway upon P5abc deletion, or that it does misfold but then refolds to the native state rapidly enough that it is not detected as a distinct phase. A control experiment in which $E^{\Delta P5abc}$ was misfolded at lower temperatures (ref *15* and see below) and then transferred to the footprinting conditions gave a refolding rate constant of 0.6 min^{-1} (data not shown), the same within error as the appearance of native ribozyme starting from the unfolded population. Thus, the misfolded ribozyme refolds fast enough under these conditions that it would not be detected even if it were formed.

To determine whether $E^{\Delta P5abc}$ can form the long-lived misfolded conformer of the wild-type ribozyme and to further explore the effects of P5abc on its formation and ultimate refolding to the native state, we measured the initial rate of formation of the native ribozyme at the lower temperature of 25 °C, shown previously to give misfolding (*15*, *33*). As expected, there were two distinct phases of native $E^{\Delta P5abc}$ ribozyme formation under these conditions, indicating that most of the ribozyme transiently misfolded (Figure 3C). The initial phase of native ribozyme formation (11 ± 3%) gave a rate constant of 0.28 ± 0.15 min^{-1}, and the second phase was ~20-fold slower (0.013 ± 0.001 min^{-1}), ultimately giving an end point that reflects equilibration of the native and misfolded conformers (*33*). The rate constant for initial folding and the fraction that folds to the native state in this process are the same within error as for the wild-type ribozyme under the same conditions (*15*). Also similar to the situation for the wild type, the Mg^{2+} concentration has only a small effect on this rate constant, with a 20-fold increase giving an only 2−4-fold increase in rate (Figure S3 of the Supporting Information). These results most simply suggest that the same or similar steps are rate-limiting for folding of the wild-type and $E^{\Delta P5abc}$ ribozymes along the pathway that avoids the misfolded conformation and that P5abc has a minimal influence on this folding transition.

Chemical Footprinting of Native and Misfolded $E^{\Delta P5abc}$ Ribozyme. To probe further the degree of similarity between

[4] Unexpectedly, reaction mixtures that were not pre-incubated with P5abc at high temperatures produced slower cleavage (0.02−0.15 min^{-1}), even when the ribozyme was allowed long folding incubations (up to 3 h at 25 °C prior to addition of P5abc at 0 °C) and long incubations with P5abc at 0 °C before addition of S* (up to 1 h). The slow substrate cleavage did not affect the results because complete progress curves were collected, allowing the fraction of native ribozyme to be determined unambiguously (see Figure S2C of the Supporting Information). We do not understand the origin of this slow cleavage; however, P5abc binding gives conformational changes of the "native" $E^{\Delta P5abc}$ that increase its enzymatic activity (*4*), and some of these may be slow at low temperatures and high Mg^{2+} concentrations. Alternatively, the less active structure may be more stable than the fully active structure at 0 °C, but with a large energy barrier between the states, such that the prefolded $E^{\Delta P5abc}$−P5abc complex remains fully active on the experimental time scale.

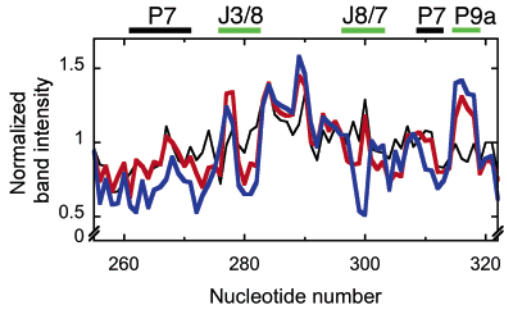

FIGURE 4: Fe(II)-EDTA footprinting of core regions of the native (blue line) and misfolded (red line) complexes of $E^{\Delta P5abc}$ with P5abc. Data for the unfolded ribozyme are also shown (black line). Differences between the native and misfolded complexes in the same regions as previously identified for the wild type are indicated with black bars (*26*), and differences that were not observed previously for the wild type are indicated with green bars.

folding of the wild-type and $E^{\Delta P5abc}$ ribozymes, we were interested in determining whether the misfolded $E^{\Delta P5abc}$ ribozyme is structurally similar to the wild-type ribozyme. Prior hydroxyl radical and DMS footprinting showed that, although the native and misfolded species of the wild type are indistinguishable over most of the sequence, there are significant differences in localized regions (*26*). Specifically, the native ribozyme is protected from hydroxyl radicals within P7 and from DMS principally within the interface of the P4−P6 and P3−P7 domains, as well as in J9.1/9.1a, which packs against P7 in the folded structure.

Populations of predominantly native or misfolded $E^{\Delta P5abc}$ ribozyme each gave hydroxyl radical footprinting patterns that were qualitatively consistent with prior experiments in which the native and misfolded species were not distinguished (*21*), with protections appearing principally within P3−P8, as well as within P2.1 and P9.1. In contrast to the wild-type ribozyme, no significant differences were observed between native and misfolded $E^{\Delta P5abc}$ ribozyme, in either hydroxyl radical or DMS footprinting experiments (Figures S4 and S5 of the Supporting Information and data not shown). This may be because the protections and enhancements are relatively weak for the $E^{\Delta P5abc}$ ribozyme (refs *21* and *33* and Figure S4 of the Supporting Information), perhaps reflecting a dynamic or "floppy" structure, which may also underlie the result that the slowest folding steps were not detected in time-resolved footprinting experiments. Further, the population of "native" $E^{\Delta P5abc}$ ribozyme actually includes ~40% misfolded ribozyme, which persists at equilibrium (*33*) and would be expected to dampen any differences in signal between the two species.

To overcome these limitations, we added P5abc to $E^{\Delta P5abc}$ in trans, trapping a complex with the misfolded ribozyme or giving an essentially homogeneous population of native ribozyme after a 50 °C incubation (*33*). Both complexes gave additional changes in hydroxyl radical footprinting, in good agreement with earlier results (ref *21* and Figures S4−S6 of the Supporting Information). Further, the differences characteristic of the native and misfolded species for the wild-type ribozyme were present for the complex, both by hydroxyl radical and DMS footprinting (Figure 4). Thus, the misfolded $E^{\Delta P5abc}$ ribozyme is rapidly converted when P5abc binds to a conformer that resembles the misfolded wild-type ribozyme, most simply suggesting that the nature of the misfolding is the same. The misfolded wild-type ribozyme was suggested to differ in topology from the native ribozyme (*26*), and this altered topology may also be present in the misfolded $E^{\Delta P5abc}$ ribozyme.

On the other hand, a small number of additional differences were observed between the native and misfolded $E^{\Delta P5abc}$ ribozyme complexes with P5abc that were not detected for the wild-type ribozyme (Figure 4 and Figures S4 and S5 of the Supporting Information). A major change is within P5, close to the connection point of P5abc in the wild-type ribozyme, suggesting that the trans complexes undergo small-scale rearrangements that are not possible when P5abc is covalently connected. A second difference is in single-stranded J8/7 segment (nucleotides 299−300), within the core, where the native complex is protected relative to the misfolded complex. Smaller differences are also present in P8, P9a, P9, and J9.1/9.1a. It is possible that rearrangements at the "broken" junction of P5abc and P4−P6 propagate through P9 to regions within the core. Alternatively, the misfolded $E^{\Delta P5abc}$−P5abc ribozyme complex may be more dynamic than the native complex and therefore give localized regions of increased solvent accessibility.

Refolding of the $E^{\Delta P5abc}$ Ribozyme from the Long-Lived Misfolded Conformer. To further explore the effects of P5abc on folding, we measured the rate of refolding of the long-lived misfolded conformer of $E^{\Delta P5abc}$. Ribozyme was folded predominantly to the misfolded species, and refolding to the native state was assessed by activity as described above [except that folding was quenched by adding P5abc and an increasing Mg^{2+} concentration at 25 °C; see Materials and Methods (*33*)]. The fraction of native $E^{\Delta P5abc}$ ribozyme increased slowly from a population of misfolded ribozyme ($k_{obs} = 0.018\ min^{-1}$), indicating net refolding of misfolded ribozyme (Figure 5A; this refolding reaction is also visible in Figure 3C as a second phase of native ribozyme formation). Consistent with previous results, this fraction was observed to plateau at a value significantly less than one, indicating that $E^{\Delta P5abc}$ equilibrates between the native and misfolded species (*33*). From the observed rate constant and the equilibrium constant calculated from the end point, the rate constant for refolding was calculated to be $0.011\ min^{-1}$, 80-fold faster than that of the wild-type ribozyme (Figure 5A). Thus, deleting P5abc destabilizes the misfolded conformation substantially relative to the transition state for refolding to the native state.

Addition of urea accelerated refolding, indicating that partial unfolding is required to refold the misfolded $E^{\Delta P5abc}$ ribozyme to the native state. The concentration dependence gave an *m* value of $-1.0\ kcal\ mol^{-1}\ M^{-1}$ in the presence of 10 or 50 mM Mg^{2+} (Figure 5B), equivalent to the exposure of ~12 bp to solvent (*40*). Thus, even without P5abc, considerable unfolding is required. Nevertheless, this *m* value is nearly 2-fold smaller than that of the wild-type ribozyme [$-1.7\ kcal\ mol^{-1}\ M^{-1}$ (ref *26* and data not shown)], indicating that, in the absence of P5abc, only approximately half as much structure becomes exposed to solvent in the transition state for refolding.

Stabilization of the Native Ribozyme by P5abc. Taken together, the results given above suggest that P5abc generally hinders folding of the ribozyme. On the other hand, it contributes significant thermodynamic stability to the folded ribozyme by stabilizing folded species relative to unfolded

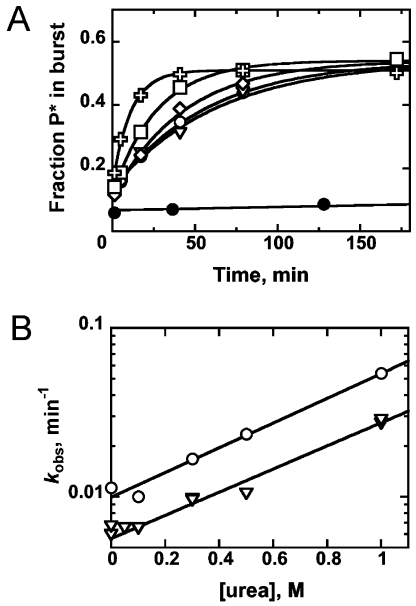

FIGURE 5: Acceleration by urea of refolding of the misfolded $E^{\Delta P5abc}$ ribozyme. (A) Time courses of refolding. Conditions and results are as follows: no urea (○), $k = 0.018$ min^{-1}; 0.1 M urea (▽), $k = 0.016$ min^{-1}; 0.3 M urea (◇), $k = 0.026$ min^{-1}; 0.5 M urea (□), $k = 0.037$ min^{-1}; and 1 M urea (crosses), $k = 0.091$ min^{-1}. Refolding of $E^{\Delta P5abc}$ in the absence of urea has been described and gave the same result within error (*33*). Refolding of the wild type in the absence of urea is also shown (●). Analysis of these and longer time points gave a k of 1.2×10^{-4} min^{-1}. All reactions were carried out at 25 °C and pH 7.0 in 10 mM Mg^{2+}. (B) Dependence of refolding rate on urea concentration [(○) $m = 1.00 \pm 0.04$ kcal mol^{-1} M^{-1}]. Analogous reactions with a higher Mg^{2+} concentration [50 mM (▽)] gave the same value within error (0.93 ± 0.05 kcal mol^{-1} M^{-1}).

ones (*19*, *21*, *33*), stabilizing the native structure relative to related but poorly active or inactive structures and thereby activating catalysis (*4*), and stabilizing the native fold relative to the long-lived misfolded structure (*33*). Here we use enzyme activity to make a distinct measurement, the fraction of $E^{\Delta P5abc}$ ribozyme present in the native (or nativelike) state as a function of Mg^{2+} concentration. Although the Mg^{2+} dependence of global structure formation has been followed by Fe(II)-EDTA footprinting (*21*, *33*), the native and misfolded species are similar in free energy at 10 mM Mg^{2+} (*33*), so these experiments presumably followed formation of a mixture of these species and may even have followed a transition predominantly to the misfolded species.

Thus, we incubated the ribozyme in varying concentrations of Mg^{2+} to allow equilibration between folding intermediates. P5abc and additional Mg^{2+} (50 mM) were added, and the fraction of native ribozyme was determined by activity. Because the ribozyme folds predominantly to the misfolded conformation in the presence of P5abc and the commitment between alternative pathways is late in folding (*28*; see Scheme 1 and Figure 7), most of the ribozyme that was unfolded or partially folded was expected to misfold upon addition of P5abc and Mg^{2+} (the small fraction expected from Figure 3C to avoid misfolding and form the native state would give a baseline value of 11% native ribozyme). In contrast, any ribozyme that was native in the initial incubation, or near-native, i.e., past the commitment point between alternative pathways, would be activated upon binding P5abc to give rapid substrate cleavage. Two determinations gave a Mg^{2+} midpoint of 2.4 ± 0.4 mM Mg^{2+} (Figure 6), the same

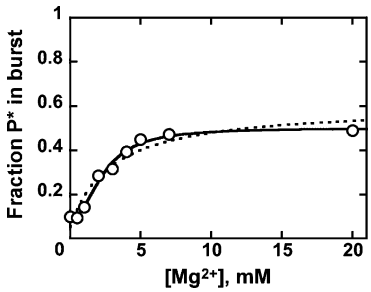

FIGURE 6: Mg^{2+} concentration dependence for native $E^{\Delta P5abc}$ ribozyme formation. Data from two independent determinations gave a $K_{1/2}$ value of 2.4 ± 0.2 mM Mg^{2+} and a Hill coefficient of 1.8 ± 0.4. The maximum fraction of native ribozyme, 0.48 ± 0.04, reflects equilibration between the native and misfolded species (*33*). The fraction of native ribozyme present at the *y*-axis (i.e., at "0" Mg^{2+}, 0.09 ± 0.02) is not zero because a small fraction of the ribozyme folds to the native state rather than misfolding upon addition of 50 mM Mg^{2+} and excess P5abc. Any ribozyme present in the native state prior to addition of P5abc produces an increase above this baseline value, as shown by the curve. Fitting the data by a simple hyperbolic binding curve (shown as a dashed curve) gave a systematic deviation from the data and a similar $K_{1/2}$ value (2.8 mM).

within error as that observed by Fe(II)-EDTA footprinting for much of the ribozyme under the same conditions (*33*). Thus, the Mg^{2+} dependence for native state formation is similar to that for global structure formation. Apparently, the misfolded species is no more stable than the native species at low Mg^{2+} concentrations, so the appearance of native ribozyme mirrors the formation of global structure. As the two structures share high degrees of global and local similarity, it is perhaps not surprising that they exhibit similar Mg^{2+} concentration dependences. As expected, the wild-type ribozyme had a much lower Mg^{2+} requirement [0.2−0.5 mM Mg^{2+} (data not shown)], similar to that determined by Fe(II)-EDTA footprinting under similar solution conditions at higher temperatures (*19*).

DISCUSSION

Using time-resolved footprinting and enzyme activity assays, we probed the effects of deleting the peripheral element P5abc throughout tertiary folding. Our results are summarized in Figure 7 [developed from previous schemes (*3*, *28*, *41*)]. Strikingly, deletion of P5abc tends to accelerate folding rather than inhibit it, and the acceleration begins at the earliest detectable formation of tertiary structure. The first region of the $E^{\Delta P5abc}$ ribozyme to become structured is the junction of P2 and P2.1, whereas P5abc and P4−P6 are the earliest for the wild type. Thus, deletion of P5abc alters the predominant pathway early in folding, giving accumulation of an intermediate that is not populated significantly by the wild-type ribozyme. Then structure forms throughout $E^{\Delta P5abc}$ on a time scale similar to the earliest protections for the wild-type ribozyme. Together, these results suggest that, although P5abc and the P4−P6 domain may provide a stable structure upon which other structure is built during folding, the partially structured intermediates that accumulate and are therefore detected experimentally do not await the formation of additional structure. Instead, they await the disruption of structure, either non-native structure or native structure that must transiently be disrupted to allow other native structure

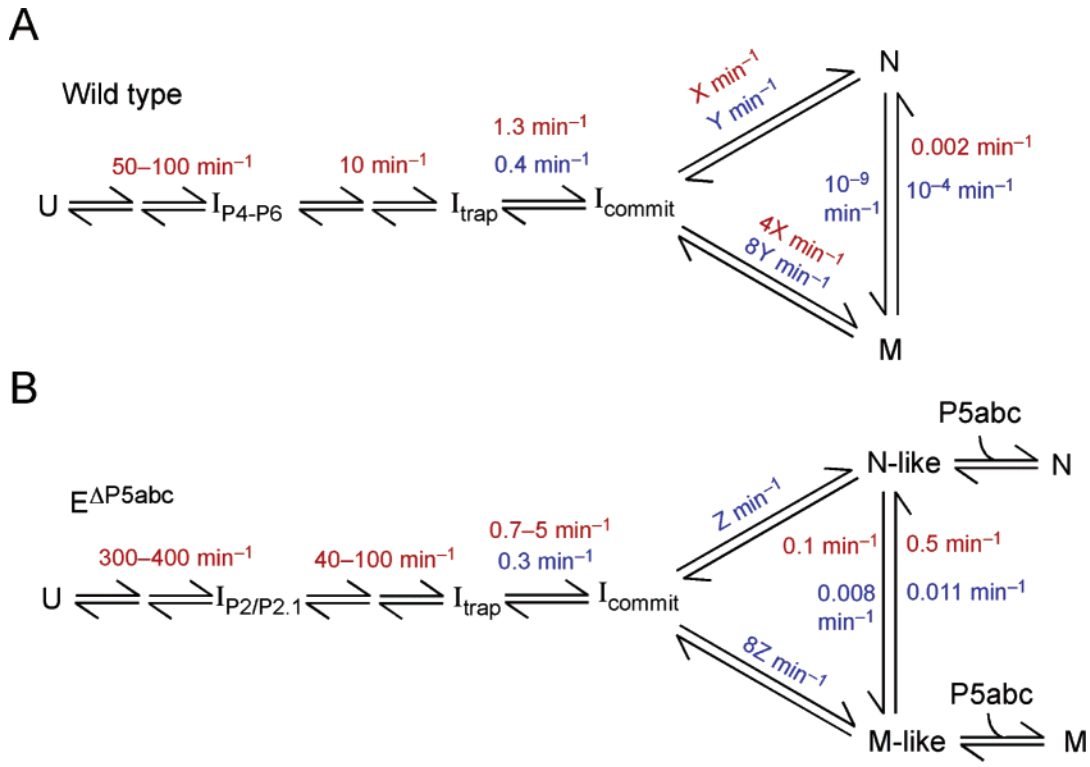

FIGURE 7: Ribozyme folding schemes for (A) the wild type and (B) $E^{\Delta P5abc}$. In each panel, rate constants measured at 42 and 25 °C are shown in red and blue, respectively. For the sake of simplicity, early folding steps are shown along a single pathway, but folding probably occurs along multiple pathways, with the pathway shown carrying the largest flux (*15*, *18*, *41*). At 25 °C, only transitions after I_{trap} are given rate constants because the earlier steps have not been measured. The commitment points between pathways to the native and misfolded species are shown late in folding for both ribozymes, as shown previously for the wild-type ribozyme (*28*) and inferred for $E^{\Delta P5abc}$ from its similar overall folding kinetics and partitioning between native and misfolded species. The slow rearrangement from I_{trap} is shown as a distinct step from the commitment to pathways (from I_{commit}) because under some conditions the wild-type ribozyme avoids I_{trap} but still gives the same partitioning between pathways (*49*). It should be emphasized that partial unfolding of I_{trap} is required for further productive folding (*17*), and I_{commit} is likely to be less structured than I_{trap} even though it is formed after I_{trap}. The rate constants for folding from I_{commit} are labeled as ratios rather than numeric values because, if the observed rate constant for folding reflects folding from I_{trap}, the data do not provide values for folding from I_{commit} to N and M; however, the ratios are constrained by the fractions that fold to the native or misfolded states. The species formed from I_{commit} for the $E^{\Delta P5abc}$ ribozyme are labeled N-like and M-like to emphasize the structural differences between the wild-type and P5abc-deleted ribozyme and the fact that the fully active native structure and the fully stable misfolded structure are not realized unless P5abc is present. Rate constants for folding from native to misfolded species are based on the kinetics and equilibria of interconversion of the two species for the $E^{\Delta P5abc}$ ribozyme and, for the wild type, on the measured rate of misfolded ribozyme refolding and the equilibrium constant calculated from the difference in binding affinity of P5abc for the native and misfolded $E^{\Delta P5abc}$ ribozyme (*33*). Under these conditions, the fastest phase of folding to the native state occurs in minutes, as shown. With bound oligonucleotide substrate or higher concentrations of monovalent ions prior to Mg^{2+} addition, bursts of native wild-type ribozyme appear on a time scale of seconds (*1*, *2*, *41*, *49*). These pathways are not shown because they are not populated significantly under these conditions.

to form. As resolution of these trapped intermediates allows folding to proceed along a pathway that ultimately gives predominantly the long-lived misfolded structure, the early traps are presumably distinct from the non-native structure and/or topology that underlies the long-lived misfolded conformation, underscoring the large number of kinetic traps in RNA folding (*16*).

It is striking that the most rapid protections for $E^{\Delta P5abc}$ occur faster even than protections for the wild type of P5abc and other parts of P4−P6. This result implies that in folding of the wild-type ribozyme, P5abc inhibits structure formation before it forms detectable tertiary structure itself. A similar observation, that P5abc is protected more rapidly as a separate molecule than within the ribozyme or the intact P4−P6 domain, previously led to a similar conclusion (*42*). It appears that a P5abc-dependent structure is formed very early in folding of the wild-type ribozyme, and this structure inhibits the formation of stable contacts within P5abc and P2/P2.1 yet does not itself give changes in accessibility to hydroxyl radicals.

How could this inhibitory structure be undetectable via footprinting? One possibility is that the inhibition arises from local structure within P5abc, which does not give a footprinting signal either because its formation does not involve significant burial of the ribose backbone or because it is already present prior to addition of Mg^{2+}. As P5abc is known to form an alternative secondary structure, and this alternative structure is influenced by the presence or absence of P4−P6 (*43*, *44*), the prior observation of inhibition of P5abc protection by the rest of the P4−P6 domain (*42*) can be rationalized by such a model.

It is more difficult to understand how local structure within P5abc could inhibit the formation of structure elsewhere in the ribozyme. An alternative is that P5abc rapidly collapses with the P4−P6 domain to form an intermediate that inhibits further folding but does not give protection from hydroxyl radicals, either because the intermediate is heterogeneous at the level of atomic contacts or it is sufficiently dynamic that no regions are strongly protected (*42*). Such a model has been proposed previously to underlie the finding that global

tertiary structure formation is accelerated by mutation of L5b or its contact partner, the receptor of J6a/6b (*29*).

In contrast to its strong effects on early folding steps, P5abc has only a small effect on the rate of overall folding to the native state for the fraction of the population that avoids the long-lived misfolded species, giving a small increase in the rate. P5abc also has a minimal effect on the partitioning between pathways to the native and misfolded species. The similarity of these folding properties and of the misfolded species, as indicated by footprinting, suggests that the folding pathways for the wild-type and $E^{\Delta P5abc}$ ribozymes are similar, as shown in Figure 7. A further similarity is that neither ribozyme gives detectable "bursts" of native ribozyme more rapidly than the time scales predicted for the pathways shown in Figure 7 (tens of seconds), indicating that "fast-track" folding pathways are not significantly populated under these conditions (*15*).

As folding of the fraction of the wild-type ribozyme that avoids the long-lived misfolded conformation is modestly accelerated by urea (*14*, *24*; H. Suh, Y. Wan, R. Russell, and D. Herschlag, manuscript in preparation), the process is apparently rate-limited by rearrangement of a kinetically trapped species (I_{trap} in Figure 7). The similar folding rate and partitioning between pathways suggest that the rate-limiting step is similar to that of the wild-type ribozyme, and the absence of a strong effect of P5abc deletion on folding from I_{trap} then suggests that P5abc does not unfold in this transition and does not stabilize the contact or contacts that are disrupted. However, it remains possible that deleting P5abc changes the nature of the rate-limiting step and coincidentally gives an overall rate constant that is similar to that of the wild type. The discontinuous activity assay developed here may be useful for probing the nature of the rate-limiting step for the $E^{\Delta P5abc}$ ribozyme by allowing examination of the dependences of the folding rate on solution conditions.

In contrast to its small effects on folding of the I_{trap} intermediate, P5abc strongly inhibits refolding of the misfolded ribozyme to the native state, implying that contacts involving P5abc are disrupted in the folding transition. Interestingly, ablation of individual tertiary contacts within P5abc gives similar accelerations (*26*), implying a high degree of cooperativity between the tertiary contacts of P5abc. It is notable that a higher Mg^{2+} concentration does not strongly inhibit refolding of the misfolded $E^{\Delta P5abc}$ ribozyme [10−50 mM (Figure 5B)], whereas dramatic inhibition is observed for the wild-type ribozyme (*28*, *45*). Several Mg^{2+} ions bind to sites within P5abc (*23*, *37*), raising the possibility that the Mg^{2+} dependence for the wild-type ribozyme arises at least in part from a requirement for dissociation of one or more of these Mg^{2+} ions.

Pros and Cons of RNA Peripheral Elements. Our results show that the presence of P5abc slows folding across a wide range of time scales, inhibiting early steps as well as later ones. The most straightforward explanation for slower folding is that P5abc forms contacts that must be disrupted for folding to proceed. Thus, the finding that even the early steps are inhibited underscores the pervasiveness of kinetic traps in folding of large RNAs, as well as suggesting that under these conditions, early formation of structure within P5abc is an impediment to the folding process rather than a benefit. It remains possible that structure within P5abc does facilitate early folding steps under solution conditions more similar to those found in vivo, i.e., with a higher monovalent ion concentration and a lower Mg^{2+} concentration, but hydroxyl radical footprinting has shown that in Na^+, even in the complete absence of Mg^{2+}, overall folding is much slower than structure formation in P4−P6 (*1*, *2*). Thus, there is no simple expectation for acceleration of early steps to accelerate overall folding. Indeed, it is reasonable to consider that peripheral structures, in general, may be deleterious for the process of RNA folding. Their presence increases the number of contact-forming regions, which increases the number of potential incorrect contacts. Further, their location on the outside of the RNA structure introduces the possibility that their formation can trap core elements outside the globular structure (*41*) or can stabilize non-native structure or topology within the core (*26*). Thus, the presence of peripheral elements strengthens the requirement for a particular order of contact formation, as well as increasing the likelihood and exacerbating the consequences of forming non-native contacts. It is perhaps not surprising that the group I intron from *Azoarcus*, which folds rapidly, lacks peripheral elements almost entirely (*46*).

In contrast to its apparent deleterious effect on the kinetics of folding, P5abc clearly provides assistance with the thermodynamics (*4*, *21*, *33*; Figure 6). This stabilization would presumably cause P5abc to be retained during evolution of group I RNAs even if it were an impediment during folding, and there may be analogous pressure for retention of other peripheral structures. One possibility is that because of the presence of RNA chaperone proteins and high counterion concentrations in vivo, there is no selective pressure for fast folding of RNAs, so there is no deleterious effect of retaining peripheral elements even if they slow folding. On the other hand, the ubiquitous involvement of DExD/H-box proteins in RNA folding and RNP biogenesis suggests that, at a minimum, RNAs misfold frequently to conformations that are sufficiently long-lived to require assistance from proteins (*47*). Thus, there may be selective pressure for RNAs to increase their folding rates by reducing the size of their peripheral structure. Consistent with this idea, some group I RNAs have apparently lost peripheral elements during evolution or replaced them with proteins (*48*). Indeed, recruitment of a protein may offer the best of both worlds; the protein could bind tightly to the native structure, stabilizing it relative to unfolded and perhaps alternative structures, while its presence as a separate molecule would minimize any deleterious effects during folding of the RNA.

ACKNOWLEDGMENT

We thank Michael Brenowitz, Sayan Gupta, and the staff of beamline X-28C (National Synchrotron Light Source, Brookhaven National Laboratory) for assistance with footprinting experiments and Michael Brenowitz, Dan Herschlag, and members of the Russell lab for helpful comments on the manuscript.

SUPPORTING INFORMATION AVAILABLE

Time-resolved synchrotron hydroxyl radical footprinting data (Figure S1), control reactions using the discontinuous assay for folding of $E^{\Delta P5abc}$ (Figure S2), comparisons of

folding reactions using discontinuous and continuous folding assays under conditions that allow the use of both assays (Figure S3), gel images from Fe(II)-EDTA and DMS footprinting of native and misfolded ribozyme species (Figure S4), quantitative results from Fe(II)-EDTA footprinting (Figure S5), and a summary of regions of the $E^{\Delta P5abc}$ ribozyme that gave Mg^{2+}-dependent changes in hydroxyl radical modification in time-resolved and equilibrium footprinting experiments (Figure S6). This material is available free of charge via the Internet at http://pubs.acs.org.

REFERENCES

1. Uchida, T., Takamoto, K., He, Q., Chance, M. R., and Brenowitz, M. (2003) Multiple monovalent ion-dependent pathways for the folding of the L-21 *Tetrahymena thermophila* ribozyme, *J. Mol. Biol. 328*, 463−478.
2. Shcherbakova, I., Gupta, S., Chance, M. R., and Brenowitz, M. (2004) Monovalent ion-mediated folding of the *Tetrahymena thermophila* ribozyme, *J. Mol. Biol. 342*, 1431−1442.
3. Sclavi, B., Sullivan, M., Chance, M. R., Brenowitz, M., and Woodson, S. A. (1998) RNA folding at millisecond intervals by synchrotron hydroxyl radical footprinting, *Science 279*, 1940−1943.
4. Engelhardt, M. A., Doherty, E. A., Knitt, D. S., Doudna, J. A., and Herschlag, D. (2000) The P5abc peripheral element facilitates preorganization of the *Tetrahymena* group I ribozyme for catalysis, *Biochemistry 39*, 2639−2651.
5. Tinoco, I., Jr., and Bustamante, C. (1999) How RNA folds, *J. Mol. Biol. 293*, 271−281.
6. Herschlag, D. (1995) RNA chaperones and the RNA folding problem, *J. Biol. Chem. 270*, 20871−20874.
7. Baldwin, R. L., and Rose, G. D. (1999) Is protein folding hierarchic? I. Local structure and peptide folding, *Trends Biochem. Sci. 24*, 26−33.
8. Gartland, W. J., and Sueoka, N. (1966) Two interconvertible forms of tryptophanyl tRNA in *E. coli*, *Proc. Natl. Acad. Sci. U.S.A. 55*, 948−956.
9. Lindahl, T., Adams, A., and Fresco, J. R. (1966) Renaturation of transfer ribonucleic acids through site binding of magnesium, *Proc. Natl. Acad. Sci. U.S.A. 55*, 941−948.
10. Walstrum, S. A., and Uhlenbeck, O. C. (1990) The self-splicing RNA of *Tetrahymena* is trapped in a less active conformation by gel purification, *Biochemistry 29*, 10573−10576.
11. Emerick, V. L., and Woodson, S. A. (1994) Fingerprinting the folding of a group I precursor RNA, *Proc. Natl. Acad. Sci. U.S.A. 91*, 9675−9679.
12. Downs, W. D., and Cech, T. R. (1996) Kinetic pathway for folding of the *Tetrahymena* ribozyme revealed by three UV-inducible crosslinks, *RNA 2*, 718−732.
13. Pan, T., and Sosnick, T. R. (1997) Intermediates and kinetic traps in the folding of a large ribozyme revealed by circular dichroism and UV absorbance spectroscopies and catalytic activity, *Nat. Struct. Biol. 4*, 931−938.
14. Treiber, D. K., Rook, M. S., Zarrinkar, P. P., and Williamson, J. R. (1998) Kinetic intermediates trapped by native interactions in RNA folding, *Science 279*, 1943−1946.
15. Russell, R., and Herschlag, D. (1999) New pathways in folding of the *Tetrahymena* group I RNA enzyme, *J. Mol. Biol. 291*, 1155−1167.
16. Treiber, D. K., and Williamson, J. R. (1999) Exposing the kinetic traps in RNA folding, *Curr. Opin. Struct. Biol. 9*, 339−345.
17. Zarrinkar, P. P., and Williamson, J. R. (1994) Kinetic intermediates in RNA folding, *Science 265*, 918−924.
18. Laederach, A., Shcherbakova, I., Liang, M. P., Brenowitz, M., and Altman, R. B. (2006) Local kinetic measures of macromolecular structure reveal partitioning among multiple parallel pathways from the earliest steps in the folding of a large RNA molecule, *J. Mol. Biol. 358*, 1179−1190.
19. Celander, D. W., and Cech, T. R. (1991) Visualizing the higher order folding of a catalytic RNA molecule, *Science 251*, 401−407.
20. Banerjee, A. R., Jaeger, J. A., and Turner, D. H. (1993) Thermal unfolding of a group I ribozyme: The low-temperature transition is primarily disruption of tertiary structure, *Biochemistry 32*, 153−163.
21. Doherty, E. A., Herschlag, D., and Doudna, J. A. (1999) Assembly of an exceptionally stable RNA tertiary interface in a group I ribozyme, *Biochemistry 38*, 2982−2990.
22. van der Horst, G., Christian, A., and Inoue, T. (1991) Reconstitution of a group I intron self-splicing reaction with an activator RNA, *Proc. Natl. Acad. Sci. U.S.A. 88*, 184−188.
23. Cate, J. H., Hanna, R. L., and Doudna, J. A. (1997) A magnesium ion core at the heart of a ribozyme domain, *Nat. Struct. Biol. 4*, 553−558.
24. Rook, M. S., Treiber, D. K., and Williamson, J. R. (1998) Fast folding mutants of the *Tetrahymena* group I ribozyme reveal a rugged folding energy landscape, *J. Mol. Biol. 281*, 609−620.
25. Treiber, D. K., and Williamson, J. R. (2001) Concerted kinetic folding of a multidomain ribozyme with a disrupted loop-receptor interaction, *J. Mol. Biol. 305*, 11−21.
26. Russell, R., Das, R., Suh, H., Travers, K., Laederach, A., Engelhardt, M., and Herschlag, D. (2006) The paradoxical behavior of a highly structured misfolded intermediate in RNA folding, *J. Mol. Biol. 363*, 531−544.
27. Pan, J., and Woodson, S. A. (1998) Folding intermediates of a self-splicing RNA: Mispairing of the catalytic core, *J. Mol. Biol. 280*, 597−609.
28. Russell, R., and Herschlag, D. (2001) Probing the folding landscape of the *Tetrahymena* ribozyme: Commitment to form the native conformation is late in the folding pathway, *J. Mol. Biol. 308*, 839−851.
29. Shcherbakova, I., and Brenowitz, M. (2005) Perturbation of the hierarchical folding of a large RNA by the destabilization of its scaffold's tertiary structure, *J. Mol. Biol. 354*, 483−496.
30. Zaug, A. J., Grosshans, C. A., and Cech, T. R. (1988) Sequence-specific endoribonuclease activity of the *Tetrahymena* ribozyme: Enhanced cleavage of certain oligonucleotide substrates that form mismatched ribozyme-substrate complexes, *Biochemistry 27*, 8924−8931.
31. Russell, R., and Herschlag, D. (1999) Specificity from steric restrictions in the guanosine binding pocket of a group I ribozyme, *RNA 5*, 158−166.
32. Huang, Z., and Szostak, J. W. (1996) A simple method for 3′-labeling of RNA, *Nucleic Acids Res. 24*, 4360−4361.
33. Johnson, T. H., Tijerina, P., Chadee, A. B., Herschlag, D., and Russell, R. (2005) Structural specificity conferred by a group I RNA peripheral element, *Proc. Natl. Acad. Sci. U.S.A. 102*, 10176−10181.
34. Das, R., Laederach, A., Pearlman, S. M., Herschlag, D., and Altman, R. B. (2005) SAFA: Semi-automated footprinting analysis software for high-throughput quantification of nucleic acid footprinting experiments, *RNA 11*, 344−354.
35. Inoue, T., and Cech, T. (1985) Secondary structure of the circular form of the *Tetrahymena* rRNA intervening sequence: A technique for RNA structure analysis using chemical probes and reverse transcriptase, *Proc. Natl. Acad. Sci. U.S.A. 82*, 648−652.
36. Herschlag, D., and Cech, T. R. (1990) Catalysis of RNA cleavage by the *Tetrahymena thermophila* ribozyme. 1. Kinetic description of the reaction of an RNA substrate complementary to the active site, *Biochemistry 29*, 10159−10171.
37. Cate, J. H., Gooding, A. R., Podell, E., Zhou, K., Golden, B. L., Kundrot, C. E., Cech, T. R., and Doudna, J. A. (1996) Crystal structure of a group I ribozyme domain: Principles of RNA packing, *Science 273*, 1678−1685.
38. Lehnert, V., Jaeger, L., Michel, F., and Westhof, E. (1996) New loop-loop tertiary interactions in self-splicing introns of subgroup IC and ID: A complete 3D model of the *Tetrahymena thermophila* ribozyme, *Chem. Biol. 3*, 993−1009.
39. Pan, J., Deras, M. L., and Woodson, S. A. (2000) Fast folding of a ribozyme by stabilizing core interactions: Evidence for multiple folding pathways in RNA, *J. Mol. Biol. 296*, 133−144.
40. Shelton, V. M., Sosnick, T. R., and Pan, T. (1999) Applicability of urea in the thermodynamic analysis of secondary and tertiary RNA folding, *Biochemistry 38*, 16831−16839.
41. Russell, R., Zhuang, X., Babcock, H. P., Millett, I. S., Doniach, S., Chu, S., and Herschlag, D. (2002) Exploring the folding landscape of a structured RNA, *Proc. Natl. Acad. Sci. U.S.A. 99*, 155−160.
42. Deras, M. L., Brenowitz, M., Ralston, C. Y., Chance, M. R., and Woodson, S. A. (2000) Folding mechanism of the *Tetrahymena* ribozyme P4−P6 domain, *Biochemistry 39*, 10975−10985.
43. Wu, M., and Tinoco, I., Jr. (1998) RNA folding causes secondary structure rearrangement, *Proc. Natl. Acad. Sci. U.S.A. 95*, 11555−11560.

44. Silverman, S. K., Zheng, M., Wu, M., Tinoco, I., Jr., and Cech, T. R. (1999) Quantifying the energetic interplay of RNA tertiary and secondary structure interactions, *RNA 5*, 1665−1674.
45. Rook, M. S., Treiber, D. K., and Williamson, J. R. (1999) An optimal Mg^{2+} concentration for kinetic folding of the *Tetrahymena* ribozyme, *Proc. Natl. Acad. Sci. U.S.A. 96*, 12471−12476.
46. Rangan, P., Masquida, B., Westhof, E., and Woodson, S. A. (2003) Assembly of core helices and rapid tertiary folding of a small bacterial group I ribozyme, *Proc. Natl. Acad. Sci. U.S.A. 100*, 1574−1579.
47. Tanner, N. K., and Linder, P. (2001) DExD/H box RNA helicases: From generic motors to specific dissociation functions, *Mol. Cell 8*, 251−262.
48. Lambowitz, A. M., Caprara, M. G., Zimmerly, S., and Perlman, P. S. (1999) in *The RNA World* (Gesteland, R. F., Cech, T. R., and Atkins, J. F., Eds.) pp 451−485, Cold Spring Harbor Laboratory Press, Plainview, NY.
49. Zhuang, X., Bartley, L. E., Babcock, H. P., Russell, R., Ha, T., Herschlag, D., and Chu, S. (2000) A single molecule study of RNA catalysis and folding, *Science 288*, 2048−2051.

BI0620149